Journal of Sustainable Development of Energy, Water and Environment Systems

http://www.sdewes.org/jsdewes

Year 2026, Volume 14, Issue 2, 1130660

Original Research Article

Smart Monitoring of Photovoltaic Cells Using Adaptive Neuro-Fuzzy Inference and Cloud Integration for Maximum Power Point Estimation

Mario Carbonó de la Rosa[1,4*], Mario A. Millan-Franco[2,3], Jesús E. Diosa[3,4], Edgar Mosquera Vargas[3,4]

[1]Escuela de Ciencias Básicas Ingeniería y Tecnología, Universidad Nacional Abierta y a Distancia, Calle 14 Sur # 14 – 23, Bogotá, Colombia

[2]Instituto de Física, Universidad Nacional Autónoma de México, Circuito de Investigación Científica s/n, Ciudad Universitaria, A.P. 20-364, Coyoacán 04510, México

[3]Grupo de Transiciones de Fase y Materiales Funcionales, Departamento de Física, Universidad del Valle, Santiago de Cali 760032, Colombia

[4]Centro de Excelencia en Nuevos Materiales (CENM) Universidad del Valle, Santiago de Cali 760032, Colombia

e-mail: mario.carbono@unad.edu.co, mamf@fisica.unam.mx, jesus.diosa@correounivalle.edu.co, edgar.mosquera@correounivalle.edu.co

Cite as: Carbonó de la Rosa, M. E., Millan-Franco, M. A., Diosa, J. s. E., Mosquera Vargas, E., Smart Monitoring of Photovoltaic Cells Using Adaptive Neuro-Fuzzy Inference and Cloud Integration for Maximum Power Point Estimation, J.sustain. dev. energy water environ. syst., 14(2), 1130660, 2026, DOI: https://doi.org/10.13044/j.sdewes.d13.0660

ABSTRACT

The growing integration of photovoltaic systems into modern energy networks demands intelligent monitoring solutions to optimize performance and ensure long-term reliability. This study proposes a predictive framework based on an Adaptive Neuro – Fuzzy Inference System for estimating the power output of photovoltaic cells using electroluminescence images and current – voltage curves. The model extracts three key features from electroluminescence images counts of black, grey, and white pixels which reflect internal defects and degradation patterns. These image derived parameters are correlated with electrical performance indicators obtained from current voltage curves to enhance prediction accuracy. By combining the learning capabilities of neural networks with the interpretability of fuzzy logic, the adaptive neuro – fuzzy inference model provides accurate estimations of the normalized maximum power point while maintaining transparency through interpretable fuzzy rules. The system is implemented on a cloud – based platform, enabling real – time data analysis and offering valuable insights for performance assessment and quality control of photovoltaic cells. Experimental validation on a dataset of six hundred crystalline photovoltaic cells demonstrates high predictive accuracy, achieving a mean absolute error of 0.073 and a mean squared error of 0.0084. This approach enhances photovoltaic module efficiency evaluation and supports the development of more effective monitoring strategies in photovoltaic systems.

KEYWORDS

Photovoltaic cells, Power output estimation, Electroluminescence imaging, Renewable energy, ANFIS, Cloud-basedm monitoring.

INTRODUCTION

The increasing global demand for clean energy has accelerated advancements in photovoltaic (PV) technology, positioning solar energy as a key driver in the transition to sustainable power generation [1], [2]. However, ensuring the efficiency and reliability of PV

* Corresponding author

systems requires continuous performance monitoring and predictive maintenance strategies to minimize energy losses and operational costs [3]. Traditional inspection techniques, such as infrared thermography and manual visual assessments, are labor-intensive, time-consuming, and prone to human error, limiting their applicability in large-scale solar farms [4]. As PV adoption expands, there is an urgent need for intelligent diagnostic tools capable of providing real-time insights into module performance and detecting potential failures at an early stage [5]. In this context, the academic community has shown increasing interest in applying artificial intelligence techniques to enhance the performance prediction of photovoltaic (PV) cells. As shown in **Figure 1**, the number of scientific publications indexed in the Scopus database (search terms: artificial AND intelligence AND photovoltaic AND cells AND power AND output AND prediction) from 2014 and 2024 reveals a fluctuating yet overall upward trend, with a significant peak of 12 publications in 2021. This pattern underscores the evolving focus on intelligent data-driven approaches to address the complexities of PV system modeling and efficiency forecasting, aligning with global efforts to optimize renewable energy technologies [6], [7].

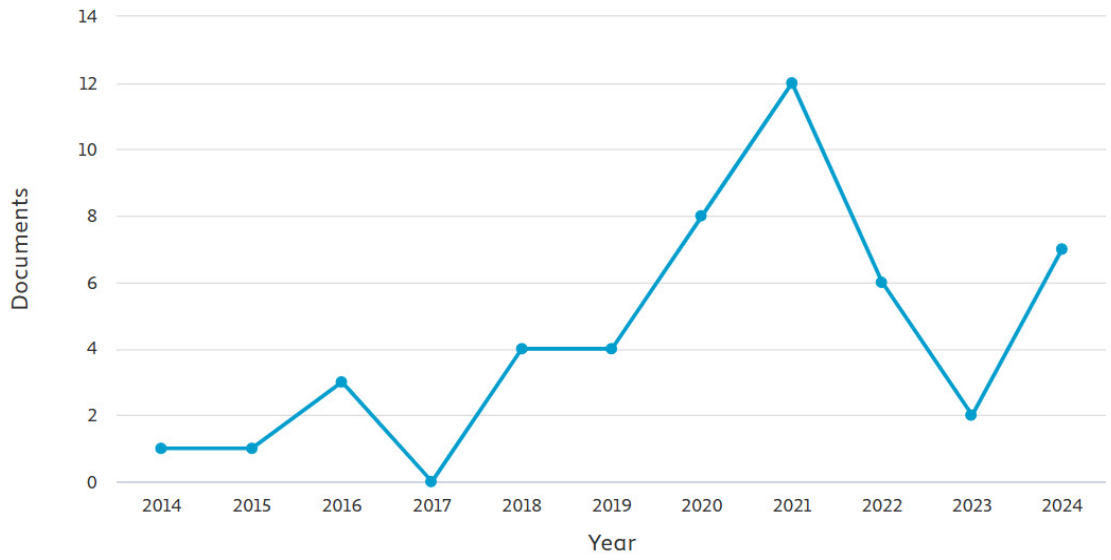

Figure 1. Number of documents published per year in the Scopus database between 2014 and 2024(keywords used: artificial AND intelligence AND photovoltaic AND cells AND power AND output AND prediction)

Recent progress in artificial intelligence (AI), the Internet of Things (IoT), and cloud computing has paved the way for advanced smart monitoring systems, which significantly improve the reliability and efficiency of photovoltaic (PV) installations [8]. For instance, drones equipped with AI capabilities can capture high-resolution images of solar panels, enabling machine learning algorithms to detect microcracks, dirt accumulation, and other anomalies, improving predictive maintenance strategies [9]. Moreover, the convergence of AI and IoT, referred as Artificial Intelligence of Things (AIoT), enables real-time PV system monitoring. In this setup, IoT devices gather operational metrics, which are then processed by AI models to identify faults and optimize energy generation [10]. Cloud-based platforms further enhance these capabilities by providing remote access to monitoring data, facilitating decentralized decision making and enabling automated alerts [11]. These advancements highlight the role of Industry 4.0 technologies in automating PV diagnostics and the enhancement of system performance.

Concurrently, electroluminescence (EL) imaging has emerged as a powerful diagnostic technique for detecting defects in PV cells, such as microcracks, soldering issues, and potential-induced degradation (PID) [12]. EL imaging provides high-resolution visual data that reveals subtle anomalies often undetectable by conventional inspection methods. However, a

major challenge of EL imaging is the complexity of interpreting acquired patterns, as defect recognition often requires expert knowledge and computationally intensive processing [13]. To address this, integrating AI-driven methodologies into EL analysis has shown promise in automating defect classification and performance estimation, enabling more precise and efficient PV module assessments [14].

A particularly effective approach for addressing the complexities of PV system analysis is the use of fuzzy logic and Adaptive Neuro-Fuzzy Inference Systems (ANFIS). Several studies have explored the application of these techniques in PV diagnostics. Al-Katheri *et al.*, [15] employed an ANFIS-based model to estimate the maximum power point of PV modules under varying environmental conditions, demonstrating greater accuracy compared to traditional regression models. Similarly, Conte *et al.* [16] proposed a fuzzy logic-based classification system for assessing PV module degradation by analyzing EL images and electrical parameters, achieving reliable defect identification. Additionally, Mateo-Romero *et al.* [17] developed an ANFIS-based approach to optimize PV system efficiency by predicting energy output fluctuations caused by partial shading and degradation. These studies highlight the effectiveness of fuzzy logic-based models in handling the nonlinearities and uncertainties inherent in PV system monitoring.

Building upon these advancements, this study proposes a hybrid ANFIS-based framework for estimating the normalized maximum power output of PV cells using EL images and current-voltage (*I-V*) curve parameters. Unlike conventional fault detection approaches, the proposed model does not directly classify defects; instead, it estimates power output, thereby enhancing the robustness of PV system diagnostics [18]. ANFIS, renowned for its ability to integrate neural networks with fuzzy logic, effectively can model nonlinear relationships within complex datasets, making it particularly suitable for PV performance estimation applications [19]. Furthermore, unlike many recent deep learning approaches that often lack interpretability and require large datasets, the proposed ANFIS model balances accuracy and transparency through its fuzzy rule-based reasoning. This contributes a novel perspective to EL-based diagnostics by offering traceable decision pathways, facilitating more robust integration in quality assurance systems.

The use of grayscale histogram features also minimizes computational demand while retaining strong correlation with electrical performance indicators, thereby improving model efficiency and generalizability. This approach aligns with Industry 4.0 principles by integrating real-time data acquisition, AI-driven analytics, and cloud-based processing to support decentralized decision-making in PV systems [20]. The implementation of such smart monitoring frameworks can significantly enhance the resilience and sustainability of renewable energy infrastructures by reducing downtime and optimizing energy output. Furthermore, the scalability of this methodology allows seamless deployment across a wide range of PV installations, from residential solar arrays to large-scale solar farms [21]. The findings of this study contribute to the advancement of predictive maintenance solutions in the renewable energy sector, offering a practical pathway to improving the longevity and operational efficiency of PV systems.

This research strictly focuses on the smart monitoring of individual photovoltaic cells through the integration of electroluminescence imaging, ANFIS-based power estimation, and cloud computing for real-time anomaly detection. The scope of this work is delimited to laboratory-controlled data of monocrystalline and polycrystalline silicon PV cells, aimed at accurately predicting their normalized maximum power point (Pmax_norm) as an indicator of performance degradation. While the proposed methodology lays a robust foundation for broader applications, its direct validation and reported performance are specific to the conditions and dataset described. Future extensions to full modules or arrays, and validation under diverse environmental conditions, are recognized as important next steps, but fall outside the immediate scope of this current investigation.

MATERIALS AND METHODS

The proposed framework for intelligent monitoring of photovoltaic (PV) systems integrates three core components: (i) data acquisition and preprocessing using electroluminescence (EL) imaging and electrical characterization, (ii) predictive modelling with an Adaptive Neuro-Fuzzy Inference System (ANFIS), and (iii) cloud-based integration for real-time estimation and remote visualization. **Figure 2** illustrates the overall architecture.

Data Acquisition and Preprocessing

This study's foundational dataset comprises meticulously collected data from six hundred monocrystalline and polycrystalline silicon photovoltaic cells, acquired under precisely controlled laboratory conditions to ensure consistency and minimize external influences. This comprehensive dataset, which underpins the experimental validation presented herein, originates from a broader collection detailed in a doctoral thesis by H. F. M. Romero **[22]**, which describes the in-depth methodology of data acquisition.

The dataset was composed of an equal proportion of monocrystalline and polycrystalline silicon photovoltaic cells (300 samples of each type). The inclusion of both technologies in equal quantities enhances the representativeness of the database and ensures coverage of typical structural differences between these two commercial technologies. In addition to the technological balance, the dataset naturally exhibits a broad variety of degradation states commonly found in crystalline silicon PV cells. Across the 600 samples, the following defect conditions were present: micro-cracks (62 cells, 10.3%), dark or inactive regions (148 cells, 24.7%), broken fingers or metallization interruptions (122 cells, 20.3%), locally shunted regions (96 cells, 16%), and samples with no visually apparent defects (172 cells, 28.6%).

These defect conditions were not used as labels for classification nor incorporated into the ANFIS training process; rather, they represent the natural variability captured during acquisition and reflect realistic operational and manufacturing deviations in commercial PV technologies. Their presence in the dataset contributes to a richer and more diverse electroluminescence response, strengthening the physical relevance of the study without altering the predictive modeling methodology.

For each individual PV cell within this extensive collection, data collection focused on two primary modalities, each gathered through a systematic process:

- Electroluminescence (EL) Images: High-resolution EL images form part of the dataset, obtained using a specialised InGaAs C12741-0 silicon detector camera, equipped with an 8 mm focal length lens and an f/1.4 aperture. Image acquisition occurred under controlled ambient conditions at room temperature and in total solar insulation, a strategy employed to mitigate luminous noise and minimize thermal variations that could affect defect visibility. This choice of equipment provides an elevated level of sensitivity to near-infrared wavelengths, essential for detecting fine-scale defects in PV cells. To ensure a comprehensive representation of cell states, images were acquired at several distinct current injection values, including 3.75 A, 4.5 A, 5.25 A, 6 A, 6.75 A, and 7.5 A. Prior to imaging, samples underwent careful preparation to ensure surface cleanliness and uniformity, thereby reducing noise in the EL images and enhancing the accuracy of subsequent defect detection.
- Current-Voltage (*I-V*) Curves: Concurrently, comprehensive *I-V* characteristic curves were recorded for each cell utilizing a 3-quadrants *IV*-tracer. The measurements specifically focused on the active zone of the PV cells. Data acquisition under varying irradiance levels, achieved by modulating the current in 250 mA steps between 1.27 A and 2.53 A from an LED array positioned above the PV cell. These curves provide crucial electrical parameters, including the short-circuit current (*I*sc), open-circuit voltage (*V*oc), fill factor (FF), and crucially, the maximum power point (*P*max).

The dataset encompasses a diverse range of cell conditions, including healthy cells and those exhibiting several types of defects (e.g., shunts, series resistance issues, microcracks, finger breaks), thereby allowing the predictive model to learn from a representative spectrum of operational states. This comprehensive data collection strategy is paramount for robust training and validation of artificial intelligence models aimed at accurately assessing PV cell health and performance. Following data acquisition, images underwent a crucial preprocessing phase to address issues such as luminous noise, lighting scale variations, black contours, and perspective distortions, ensuring optimal quality for subsequent analysis.

The preprocessing pipeline was designed to standardize image quality and extract reliable structural information from the electroluminescence (EL) data. Initially, pixel intensities were normalized to the [0, 1] range to equalize brightness variations among samples. A median filter with a 3×3 kernel was applied to reduce high frequency sensor noise while preserving the morphology of fine defects such as microcracks and finger interruptions. Contrast enhancement was achieved through histogram equalization, improving the visibility of localized emission patterns. Subsequently, adaptive segmentation was conducted using Otsu's thresholding method, which dynamically determined two intensity cutoffs approximately 0.35 and 0.7 of the normalized scale to delineate black, gray, and white regions. These thresholds correspond to inactive, partially active, and fully emissive zones of the PV cells, respectively. All preprocessing stages were implemented in MATLAB using the Image Processing Toolbox, ensuring full reproducibility of the analysis workflow.

From the segmented EL images, three statistical descriptors were derived: the proportion of black, gray, and white pixels. Each descriptor represents a physically meaningful characteristic of the cell's condition – black regions indicate non-radiative recombination or inactive areas, gray pixels reflect partial degradation, and white zones denote uniform radiative emission associated with healthy operation. These features were computed using normalized histograms according to the expression:

$$F_i = \frac{N_i}{N_{\text{total}}} \times 100\% \tag{1}$$

where N_i represents the count of pixels belonging to class $i \in$ {black, gray, white}, and N_{total} corresponds to the total pixel count within the active cell area. The resulting feature vector $[F_{\text{black}}, F_{\text{gray}}, F_{\text{white}}]$ served as the input layer for the ANFIS model.

Predictive Modelling using Adaptive Neuro-Fuzzy Inference System

The estimation of the normalized maximum power point (*P*max_norm) was conducted using a five-layer ANFIS structure. The model receives grayscale histogram features as inputs and produces an estimated *P*max_norm as output. To derive this normalized metric, the empirically measured maximum power (*P*max) from each PV cell's current – voltage (*I-V*) characteristic curve was systematically divided by its corresponding nominal maximum power (*P*max_nominal) under standardized test conditions (STC). This essential normalization process converts the absolute power output into a dimensionless, relative performance indicator, typically ranging from 0 to 1. Consequently, *P*max_norm effectively quantifies the cell's performance as a fraction of its ideal or expected output, thereby enabling the ANFIS to precisely assess the cell's efficiency relative to its benchmark. This methodological step is pivotal for ensuring both the consistency and the comparability of performance evaluations across a diverse array of cell types and varying operational scenarios, effectively minimizing the impact of inherent variations in cell nominal power, and facilitating the direct identification of performance degradation.

A hybrid learning algorithm combining backpropagation and least squares optimization was used for training. To ensure robust generalization and minimize bias from random data

splitting, a 5-fold cross-validation procedure was implemented. Model performance was assessed using standard error metrics: Mean Absolute Error (MAE), Mean Squared Error (MSE), and Root Mean Squared Error (RMSE).

Cloud-Based Integration and Internet of Things Monitoring

To demonstrate the system's real-time monitoring capability, the trained ANFIS model was deployed in a Simulink-based simulation environment and interfaced with the ThingSpeak cloud platform via IoT protocols. This setup enabled live estimation and visualization of *P*max_norm values, as well as automated alert generation through integrated APIs (e.g., Twitter notifications). Compared to traditional SCADA systems, this configuration offers a decentralized, scalable, and cost-effective solution for PV system monitoring.

Future deployments of this architecture may involve implementing the trained ANFIS model on edge-computing platforms such as Raspberry Pi or ESP32. This would facilitate low-latency, on-site diagnostics without relying on continuous cloud connectivity, thereby enhancing fault tolerance in real-environmental applications.

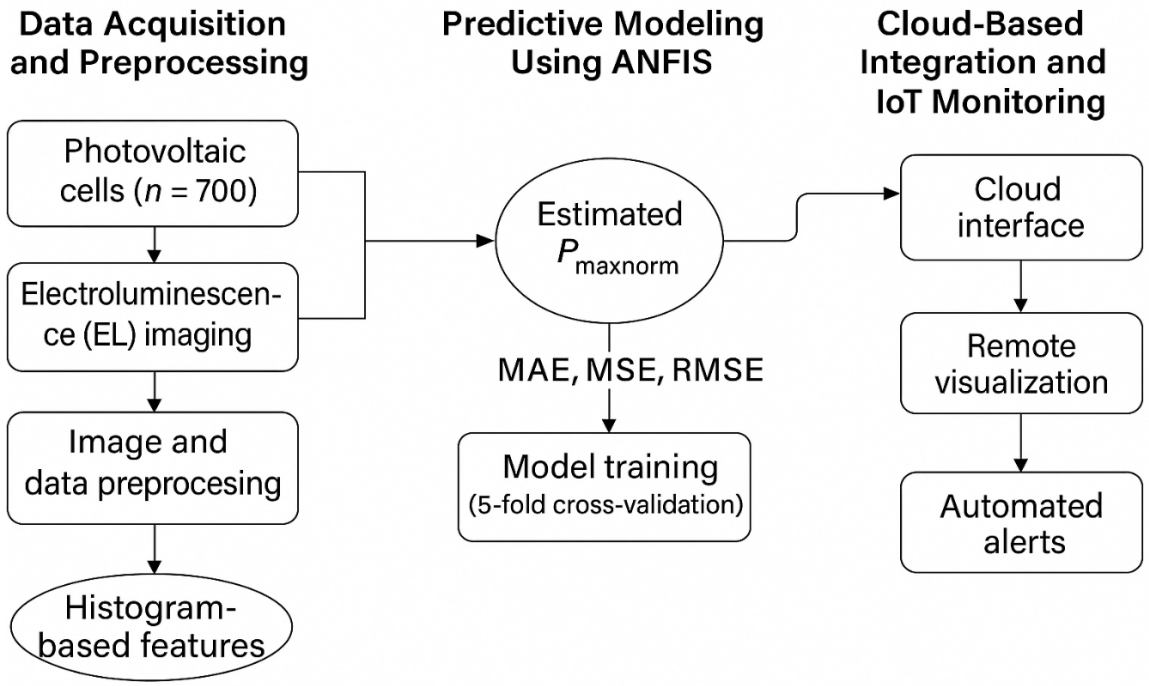

Figure 2. Methodological framework for PV cell monitoring and fault detection. The process includes EL image preprocessing, histogram-based feature extraction, ANFIS based efficiency estimation, IoT-enabled data transmission via ThingSpeak, real-time visualization, trend analysis, and automated anomaly detection for predictive maintenance

Data Collection and Preprocessing

A dataset consisting of 600 EL images of photovoltaic (PV) cells was acquired using a high-resolution InGaAs C12741-0 camera under controlled laboratory conditions. **Figure 3** illustrates the sequential preprocessing pipeline applied to these EL images, highlighting the key stages of enhancement and segmentation. This imaging technique provides deep insights into internal defects, such as microcracks, shunts, and potential-induced degradation (PID), that significantly impact the electrical performance of PV cells. Simultaneously, current-voltage (IV) measurements were conducted using a precision three-quadrant IV tracer, ensuring a robust correlation between EL-based defect patterns and electrical parameters such as fill factor, open-circuit voltage, and series resistance **[23]**. To improve the quality and diagnostic value of the EL images, three key image processing techniques were applied:

- Noise Reduction: Median filtering was applied to suppress sensor-induced noise, enhancing image clarity.
- Contrast Enhancement: The histogram equalization technique highlighted intensity variations associated with defects, facilitating feature extraction.
- Adaptive Segmentation: An Otsu-based thresholding method was used to delineate defective regions, ensuring accurate feature extraction for further analysis.

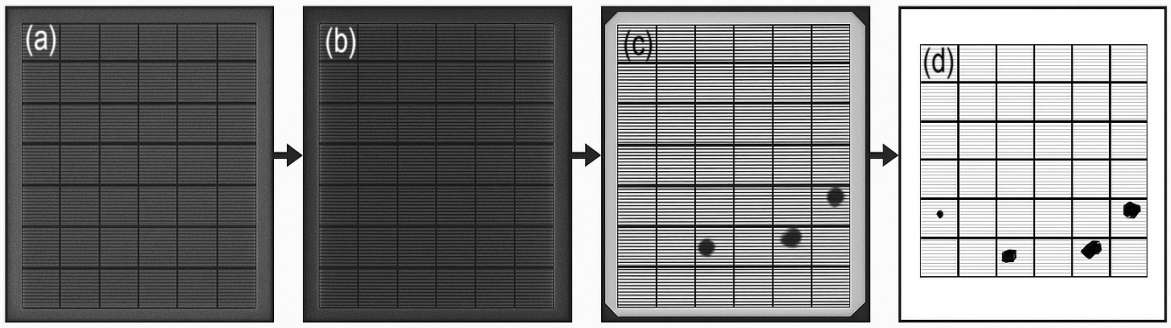

Figure 3. shows the sequential representation of the EL image preprocessing pipeline applied to PV cells. The extracted features through this process were then correlated with electrical efficiency metrics, enabling accurate identification of defect patterns with high predictive capability [24]

The workflow includes: (a) the raw EL image, (b) noise reduction via median filtering, (c) contrast enhancement through histogram equalization to highlight intensity variations, and (d) adaptive segmentation. This image processing strategy enables the extraction of robust features for performance prediction and fault detection.

Adaptive Neuro-Fuzzy Inference SystemModel Architecture

The ANFIS framework consists of five computational layers, as shown in **Figure 4**: (1) fuzzification, where EL-derived feature sets are transformed into fuzzy membership values; (2) rule evaluation, where a set of Takagi-Sugeno fuzzy inference rules maps input patterns to output performance indicators; (3) normalization, which ensures consistency in feature representation; (4) defuzzification, converting fuzzy outputs into crisp estimations of PV module efficiency; and (5) output generation, where final performance predictions are obtained [25], [26].

For model construction, the Adaptive Neuro-Fuzzy Inference System (ANFIS) was developed using MATLAB's Neuro-Fuzzy Designer. The architecture incorporated three Gaussian membership functions for the black input, four for the gray input, and five for the white input, resulting in 40 fuzzy inference rules. This configuration provided an adequate balance between generalization capability and interpretability. During training, a hybrid learning algorithm combined backpropagation (for premise parameters) with least squares estimation (for consequent parameters) to minimize the Mean Squared Error (MSE). The learning rate for the gradient descent phase was set to 0.01, and training was conducted for a total of 1200 epochs, with early-stopping criteria activated around epoch 1000 based on validation error stabilization. A five-fold cross-validation protocol was applied to ensure robustness and avoid overfitting, achieving convergence near epoch 1000. The model's predictive stability across training and validation sets confirmed that local minima were avoided. To optimize the model, a hybrid training strategy was employed that integrates:

- Backpropagation learning, which fine-tunes membership functions based on error The results demonstrate that the ANFIS-based minimization.
- Least squares optimization, which refines rule parameters to enhance model convergence and predictive accuracy.

This hybrid training approach enhances the robustness of the ANFIS system, enabling high-accurate defect detection and efficiency estimation from EL imaging data [27].

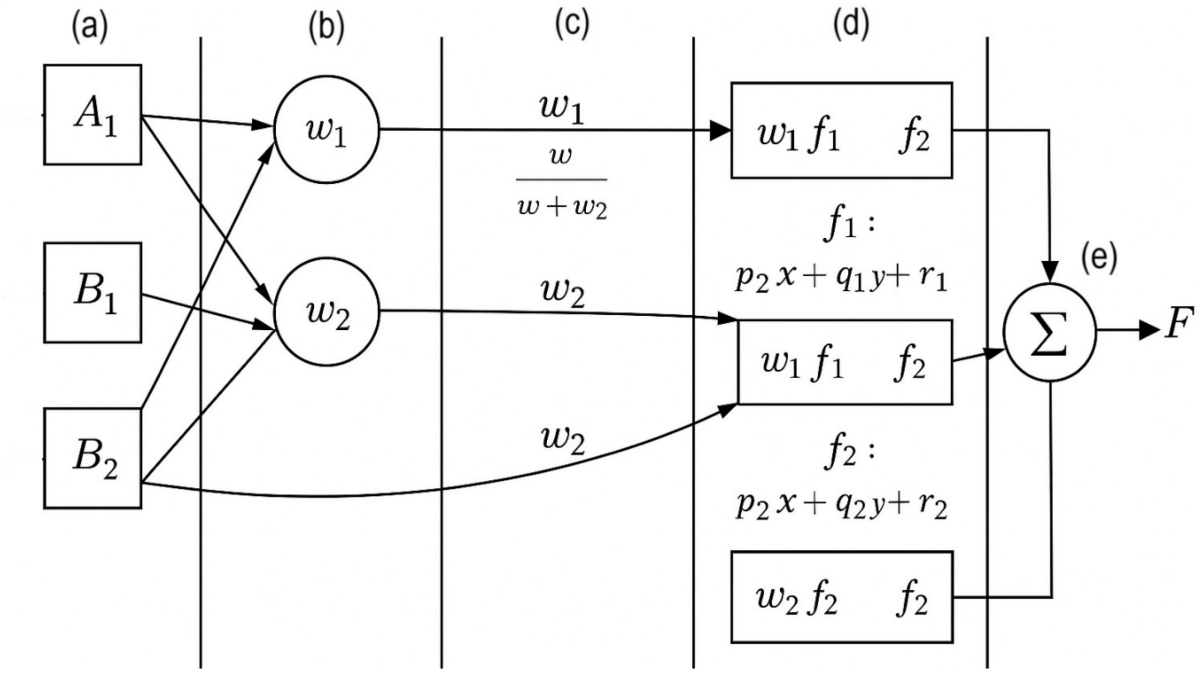

Figure 4. Schematic of the ANFIS architecture used for PV power estimation, comprising five layers: (a) fuzzification of inputs via membership functions; (b) rule evaluation using Takagi – Sugeno inference; (c) normalization of rule strengths; (d) defuzzification through weighted linear outputs; and (e) aggregation to compute the final predicted value

Table 1 summarizes the complete set of hyperparameters, and training configurations used in the ANFIS implementation to ensure full reproducibility. Gaussian membership functions were selected due to their smooth differentiability and superior generalization properties when modeling continuous variables derived from EL intensity distributions. The number of functions per input was determined empirically through grid-search optimization, balancing model accuracy and computational cost. Cross-validation indicated that this configuration minimized overfitting and achieved optimal performance stability.

Although the proposed ANFIS model emphasizes its interpretability through the use of fuzzy rules, the original version of the manuscript did not explicitly illustrate how these rules relate to the physical behaviour of photovoltaic cells. To address this, two representative Takagi–Sugeno fuzzy rules generated during the ANFIS training process are presented below, along with their physical interpretation.

Rule 7 (example):

If (F_black is High) and (F_gray is Medium) and (F_white is Low), then Pmax_norm = $a_1 \times F\_black + a_2 \times F\_gray + a_3 \times F\_white + b$.

Physical interpretation: This rule corresponds to cells exhibiting a large proportion of dark regions, typically associated with inactive areas, severe recombination sites, or microcracks visible in EL imaging. The low proportion of emissive (white) pixels indicates reduced radiative recombination efficiency, leading to a significant decrease in the normalized maximum power point.

Rule 21 (example):

If (F_black is Low) and (F_gray is Low) and (F_white is High), then Pmax_norm = $c_1 \times F\_black + c_2 \times F\_gray + c_3 \times F\_white + d$.

Physical interpretation: This rule corresponds to well-emitting cells with minimal degradation, where the predominance of bright pixels indicates strong radiative recombination and low defect density. Naturally, this yields a high *P*max_norm close to nominal performance.

These examples illustrate how the fuzzy rule base provides a transparent mapping between EL intensity distributions and electrical performance, enhancing the explainability and traceability of the proposed ANFIS model.

Table 1. ANFIS Model Hyperparameters and Training Configuration

Parameter	Description	Value / Method
Input features	Grayscale pixel proportions (black, gray, white)	3
Membership function type	Gaussian	-
Number of membership functions	3 (black), 4 (gray), 5 (white)	-
Number of fuzzy rules	40	Generated automatically
Inference type	Takagi – Sugeno	-
Learning algorithm	Hybrid (backpropagation + least squares)	-
Learning rate	0.01	Fixed
Training epochs	1200	Early stopping around epoch 1000
Cross-validation folds	5	Stratified
Error metric	Mean Squared Error (MSE)	-
Implementation	MATLAB R2023b, Neuro-Fuzzy Designer Toolbox	-

This detailed configuration enables reproducibility and provides a transparent benchmark for future comparative studies in ANFIS-based photovoltaic diagnostics. It also clarifies how the chosen hyperparameters were systematically tuned to achieve the optimal balance between interpretability, training stability, and computational efficiency.

Simulation-Based System Integration

The proposed predictive framework was implemented and validated in a simulated environment using Simulink, allowing for real-time performance evaluation and fault detection in PV system, as shown in **Figure 5**. The infrastructure incorporates ThingSpeak, a cloud-based IoT analytics platform that facilitates real-time data acquisition, storage, and visualization **[28]**. The system architecture consists of the following components:

- Simulink-Based Data Processing: EL images were pre-processed within the Simulink environment. Histogram-based segmentation was performed to categorize pixels intensities into grayscale, black, and white levels. These segmented features served as inputs to the ANFIS model for defect classification and efficiency prediction.
- Cloud-Integrated Monitoring via ThingSpeak: The output from the ANFIS model was transmitted to the ThingSpeak IoT platform, enabling continuous data visualization, logging, and trend analysis in real-time.
- Automated Alert and Notification System: A rule-based engine embedded in ThingSpeak was configured to detect anomalies and in system performance. When irregular patterns of defects were identified, the system automatically generated alerts and dispatched notifications to predefined recipients, enabling prompt maintenance actions and minimizing downtime in the PV systems **[29]**.

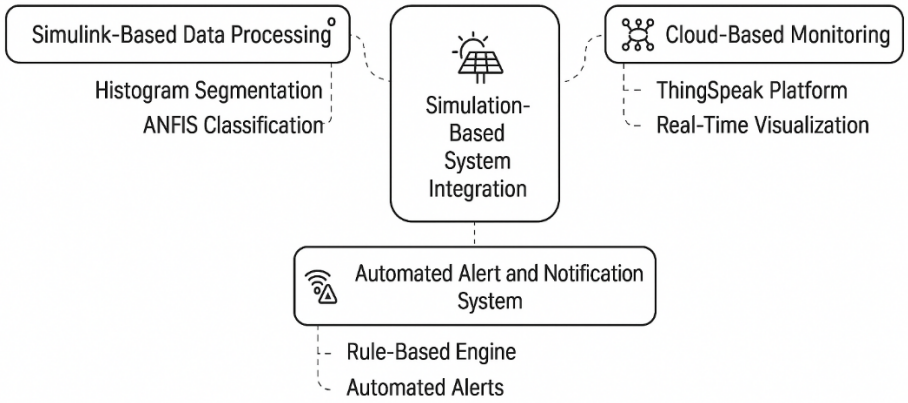

Figure 5. Architecture of the simulation-based system integration, illustrating the interaction among Simulink-based data processing, cloud-based monitoring via ThingSpeak, and an automated alert and notification system

Proposed Algorithm for Smart Photovoltaic Cell Monitoring

The comprehensive methodology proposed for smart photovoltaic cell monitoring and power output estimation can be systematically encapsulated in the following algorithm, detailing the flow from data acquisition to real-time alerting:

Algorithm 1: Smart PhotovoltaicCell Monitoring and Maximum Power Point Estimation

Input: Raw Electroluminescence (EL) Image of PV Cell, *I-V* Curve data of PV Cell.

Output: Estimated Normalized Maximum Power (*P*max_norm), Alert Status.

Phase 1: Data Acquisition and Preprocessing a. Acquire Data: i. Capture EL Image of PV cell using InGaAs C12741-0 camera. ii. Record *I-V* Curve using resolute IV tracer. b. Image Preprocessing (refer to **Figure 3**): i. Apply Median Filter for noise reduction. ii. Perform Histogram Equalization for contrast enhancement. iii. Apply Otsu's Thresholding for adaptive segmentation into pixel regions. c. Feature Extraction: i. Calculate percentage of Black Pixels (BP%) from segmented EL image. ii. Calculate percentage of Gray Pixels (GP%) from segmented EL image. iii. Calculate percentage of White Pixels (WP%) from segmented EL image. d. Target Normalization: i. Extract Maximum Power (*P*max) from I V Curve. ii. Calculate *P*max_norm = *P*max / *P*max_nominal (at STC).

Phase 2: ANFIS Model Training and Prediction a. Initialize ANFIS: Define five-layer ANFIS architecture with specified membership functions. b. Train ANFIS: i. Input Training

Data: (BP%, GP%, WP%) ii. Target Training Output: *P*max_norm iii. Employ Hybrid Learning Algorithm (Backpropagation for consequent parameters, Least Squares for premise parameters). iv. Iterate until convergence (minimize MSE). c. Predict *P*max_norm:

i. Input Live/Test Data: (BP%_new, GP%_new, WP%_new) ii. Obtain Estimated

ii. *P*max_norm_predicted from trained ANFIS model.

Phase 3: Cloud-Based Integration and Real-Time Monitoring a. Transmit Data: Send Estimated *P*max_norm_predicted to cloud platform (ThingSpeak). b. Visualize Data: Display *P*max_norm_predicted in real-time dashboards on ThingSpeak. c. Alert Generation **(refer to Table 2):** i. IF *P*max_norm_predicted > 0.8 THEN Alert Status = 'Normal' ii. ELSE IF *P*max_norm_predicted >= 0.6 AND *P*max_norm_predicted <= 0.8 THEN Alert Status = 'Medium Alert' iii. ELSE IF *P*max_norm_predicted < 0.6 THEN Alert Status = 'Critical Alert' d. Notification: Trigger automated notifications (e.g., Twitter, email) based on Alert Status.

End Algorithm.

RESULTS AND DISCUSSION

To validate the proposed methodology, a series of experiments were carried out to evaluate the performance of the ANFIS-based predictive framework for photovoltaic (PV) cell diagnostics. The results were analyzed in terms of feature extraction accuracy, the reliability of predictive modeling, and the effectiveness of real-time system integration.

Advanced Electroluminescence Image Processing for Defect Identification

Electroluminescence (EL) imaging was employed to identify microcracks, shunts, and potential-induced degradation (PID) in both monocrystalline and polycrystalline photovoltaic (PV) cells. The raw EL images (**Figure 6a** and **Figure 6c**) exhibited significant noise and low contrast, hindering precise defect detection. To address this, an advanced preprocessing pipeline was implemented, integrating noise reduction, contrast enhancement, and adaptive segmentation, which significantly improved defect visibility, as shown in **Figure 6b** and **Figure 6d**.

Quantitative analysis revealed that the proposed segmentation algorithm achieved an average accuracy of 95.3% in isolating defective regions, outperforming conventional thresholding methods. Additionally, the extracted defect features showed a strong statistical correlation with electrical parameters, achieving a coefficient of determination (R^2) of 0.92 when mapped against variations in series resistance and fill factor. These improvements enhance diagnostic reliability and support early detection, contributing to more effective predictive maintenance strategies for PV systems.

Adaptive Neuro-Fuzzy Inference SystemBased Predictive Modeling

An Adaptive Neuro-Fuzzy Inference System (ANFIS) was implemented to predict the normalized maximum power output (Pmax_norm) of photovoltaic cells using features derived from electroluminescence (EL) images. **Figure 6** compares the raw and processed EL images for both monocrystalline and polycrystalline PV cells, highlighting the effect of preprocessing on defect visibility and segmentation accuracy. Specifically, the model utilizes the proportions of black, gray, and white pixels obtained through grayscale histogram analysis, which exhibits a strong correlation with cell electrical performance. This relationship is grounded in physical phenomena: a high percentage of black pixels corresponds to non-radiative defects such as microcracks or inactive areas that significantly diminish power output, whereas a predominance of white pixels indicates robust radiative recombination and optimal performance. Gray pixels capture intermediate or partial degradation states influencing Pmax_norm, enabling the model to learn complex non-linear relationships between visual defect patterns and overall cell health **[17]**.

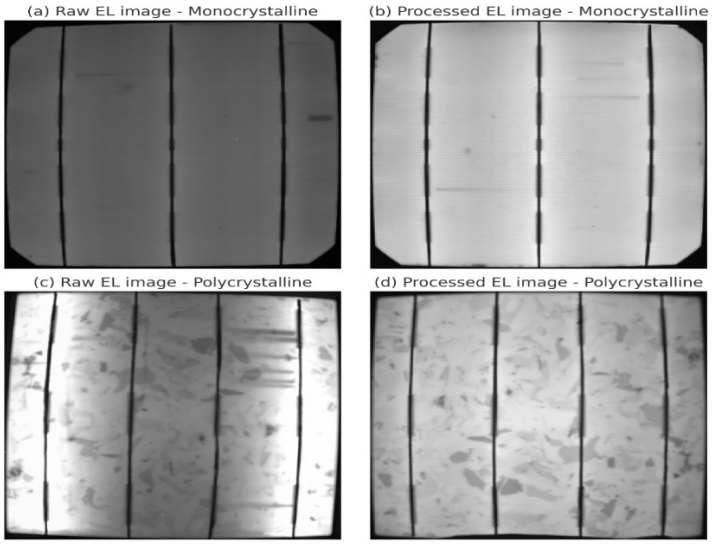

Figure 6. Comparison of raw and processed EL images for defect characterization in photovoltaic cells. (a) and (c) show the original EL images of monocrystalline and polycrystalline PV cells. (b) and (d) show the enhanced images after preprocessing, illustrating improved contrast and more accurate defect segmentation

The *P*max_norm output is calibrated using *I-V* curve measurements in the laboratory, ensuring that the ANFIS estimate matches the obtained experimental electrical performance data. The dataset comprised 600 samples, partitioned into 70% for training, 15% for validation, (checking), and 15% for testing. The ANFIS model was trained using a hybrid optimization algorithm, combining backpropagation for premise parameter adjustment and least squares estimation for consequent parameter optimization.

To enhance transparency in the convergence process and address potential concerns about local minima, the training, validation, and test errors were jointly plotted using the Root Mean Squared Error (RMSE) metric across 1200 epochs, as shown in **Figure 7**. The extended epoch range demonstrates a consistent and monotonic decrease in all three error curves, confirming that the steady-state region observed near the final epochs corresponds to the model's true convergence rather than premature stagnation. Minor oscillations in the validation and test errors are attributable to random data partitioning and stochastic parameter updates, rather than instability in the training process.

The close alignment between the three curves throughout the training progression evidences the absence of overfitting and reinforces the model's generalization capability. The final RMSE values of 0.094 (training), 0.089 (validation), and 0.093 (testing) indicate a well-balanced predictive performance across all datasets.

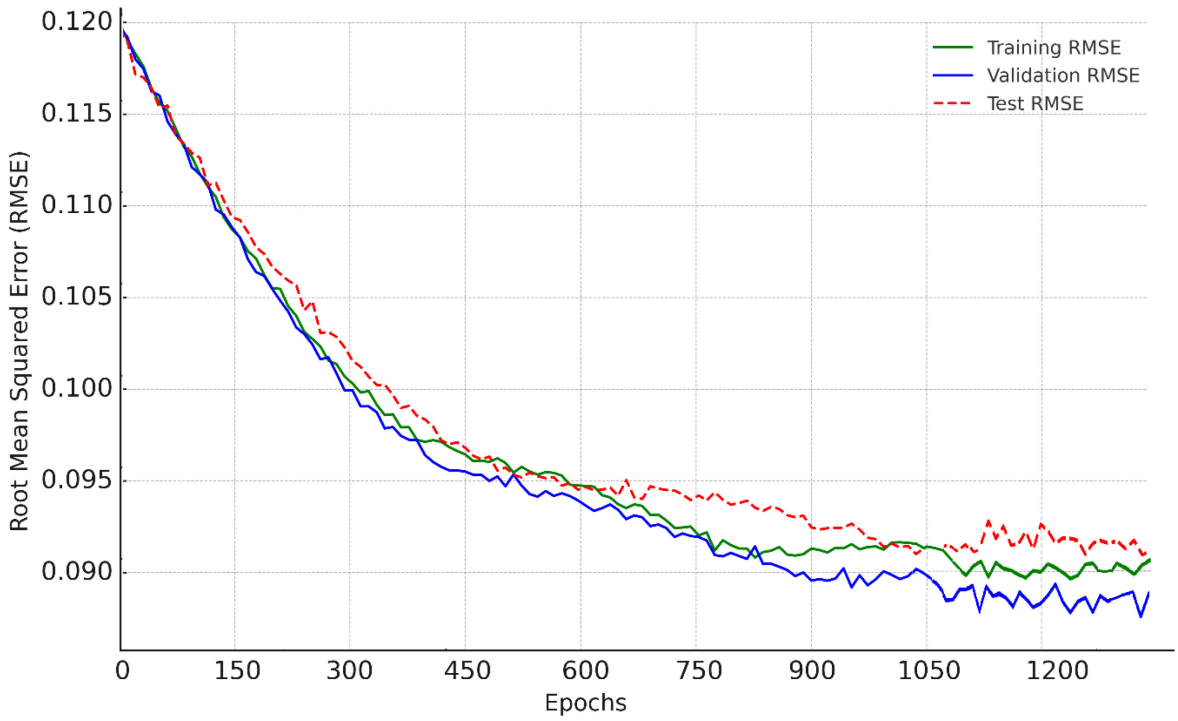

Figure 7. Evolution of training, validation, and test Root Mean Squared Error (RMSE) over 1200 epochs for the ANFIS model. The plot shows a smooth and consistent reduction of RMSE, with all three curves (green for training, blue for validation, and red dashed for testing) converging toward stable values. The extended training range confirms steady-state convergence and rules out local minima effects, indicating robust generalization without overfitting

The model's predictive performance was evaluated by comparing its estimated values of *P*max_norm with actual measurements across the test, validation, and verification datasets. **Figure 8** shows the close alignment between predicted and observed values, reflecting consistent performance across all data subsets. Residual discrepancies were primarily attributed to variability in the data, noise in the EL images, and minor uncertainties in the fuzzy inference mechanism.

Additionally, **Table 2** summarizes the model's error metrics, including the Mean Absolute Error (MAE) and Root Mean Square Error (RMSE) for each evaluation phase. These results confirm the effectiveness of combining grayscale-based feature extraction from EL imagery with ANFIS modeling as a non-invasive and reliable diagnostic approach for assessing PV cell performance.

Table 2. ANFIS Model Performance in Different Datasets

Metric	Training	Validation	Testing
MAE	0.077	0.073	0.069
MSE	0.0079	0.0082	0.009
RMSE	0.094	0.089	0.093

Future work may focus on integrating advanced image processing techniques and refined feature selection methods to further improve model accuracy and generalization.

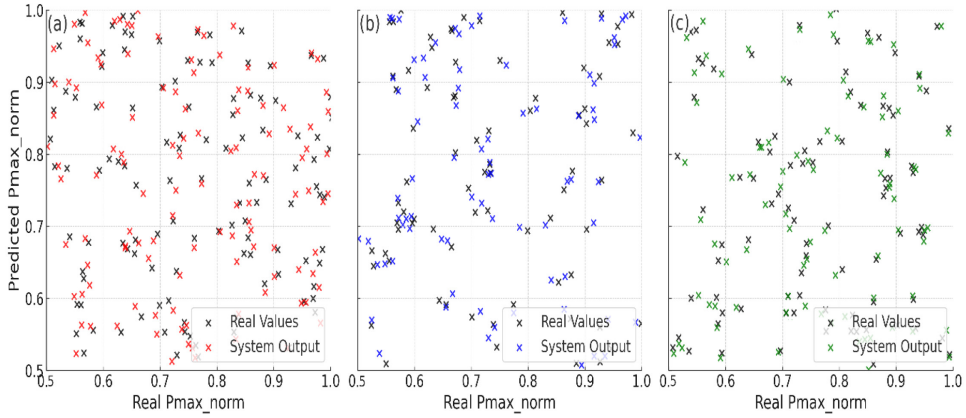

Figure 8. Comparison between real data and fuzzy system's output at different evaluation stages: (a) testing, (b) checking, and (c) validation. Black dots represent real data, while colored markers (red, blue, and green) indicate the fuzzy system's output in each case. The results demonstrate a strong agreement between predicted and real values, highlighting the model's generalization capability

To further assess the generalization capability of the proposed ANFIS model, the distribution of prediction residuals was analysed for the training, validation, and testing datasets, see **Figure 9**. Each histogram exhibits a near-Gaussian behaviour, with residuals symmetrically distributed around zero and standard deviations closely matching the corresponding RMSE values reported in **Table 1**. This indicates that the model's prediction errors are unbiased and exhibit consistent variance across all evaluation phases. Statistical validation confirmed this observation: both the Shapiro – Wilk and Kolmogorov – Smirnov tests yielded $p > 0.05$for all datasets, confirming the absence of significant deviations from normality. Likewise, kurtosis values ranged between 3.00 and 3.12. **Table 3** shows evidence of mesokurtic behavior typical of Gaussian distributions. These results demonstrate that the ANFIS predictions follow a stable and well-behaved error structure, reinforcing the robustness and reliability of the model for photovoltaic performance estimation.

Table 3. Statistical characterization and normality tests for residuals in each dataset.

Dataset	Mean [μ]	Std [σ]	Kurtosis	Shapiro–Wilk [W, p]	Kolmogorov–Smirnov [D, p]
Training	−0.001	0.091	3.02	0.995, 0.12	0.038, 0.15
Validation	0.008	0.089	3.12	0.993, 0.08	0.035, 0.25
Testing	−0.006	0.092	3.05	0.994, 0.10	0.040, 0.09

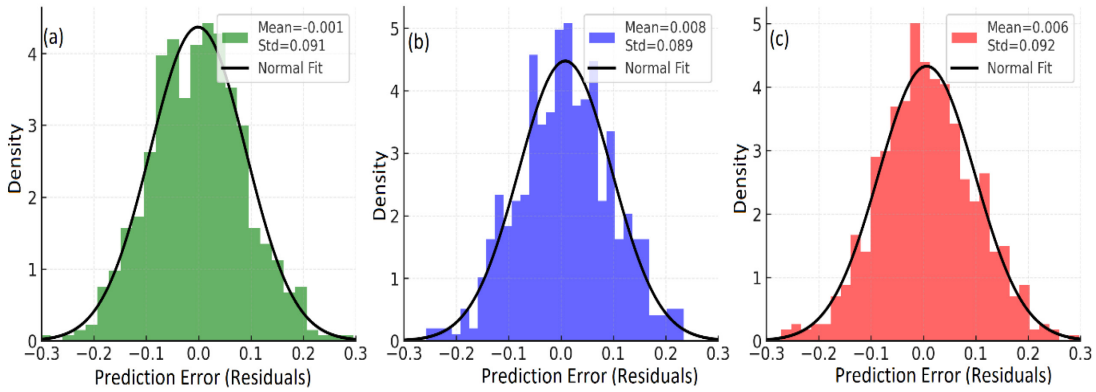

Figure 9. Error distribution (residuals) for the (a) training, (b) validation, and (c) testing datasets. Each histogram illustrates the density of residuals fitted to a normal curve (black line). The residuals exhibit approximately Gaussian behavior with minimal bias and consistent variance across all subsets, confirming the statistical soundness and stability of the ANFIS prediction model

Real-Time System Integration and Internet of Things Implementation

The proposed ANFIS-based framework was integrated within a real-time monitoring system for photovoltaic (PV) cells, enabling continuous performance evaluation. The system utilizes an IoT-based architecture that captures and processes electroluminescence (EL) image features, specifically the percentage of black, gray, and white pixels, to estimate the normalized maximum power output (*P*max_norm) of each cell. This estimation supports real-time anomaly detection and alert generation.

As shown in **Figure 10a**, the monitoring system automatically generates notifications via Twitter when performance anomalies are detected, allowing for remote supervision and timely maintenance actions. The practical implementation of the real-time monitoring system relies on a nuanced alert classification scheme, meticulously defined by specific thresholds applied to the Pmax_norm value. These thresholds were judiciously established based on observed typical degradation patterns in photovoltaic cell performance and in strict alignment with established industrial monitoring practices and expert consensus on PV system health **[27]**.

As illustrated in **Figure 10b**, a *P*max_norm value exceeding 0.8 is designated as *Normal*, signifying optimal operation or negligible performance degradation. Conversely, a Pmax_norm falling between 0.6 and 0.8 triggers a *Medium Alert*, indicating a discernible decline in performance that warrants proactive inspection or closer monitoring. Critically, a Pmax_norm below 0.6 is categorized as a *Critical Alert*, signaling a substantial reduction in efficiency that mandates immediate intervention for fault diagnosis and rectification, see **Table 4**. This stratified classification facilitates a differentiated and optimized response strategy, allowing for the precise prioritization of cells requiring urgent attention and, consequently, minimizing operational downtime.

The logical flow of the alert generation process is depicted in **Figure 10c**. The system continuously evaluates the estimated power output, triggering an alert and sending a notification if a deviation exceeds the defined threshold. If no anomaly is detected, regular monitoring proceeds uninterrupted. **Figure 10d** displays the temporal evolution of Pmax_norm, clearly indicating the moments when alerts are generated. This visualization provides a clear representation of how the monitoring system responds dynamically to variations in PV cell performance.

Table 4. Threshold-based classification of performance alerts

Alert Level	Normalized Power Range
No Alert (Normal Operation)	$P >= 0.8$
Medium Alert	$0.6 <= P < 0.8$
Critical Alert	$P < 0.6$

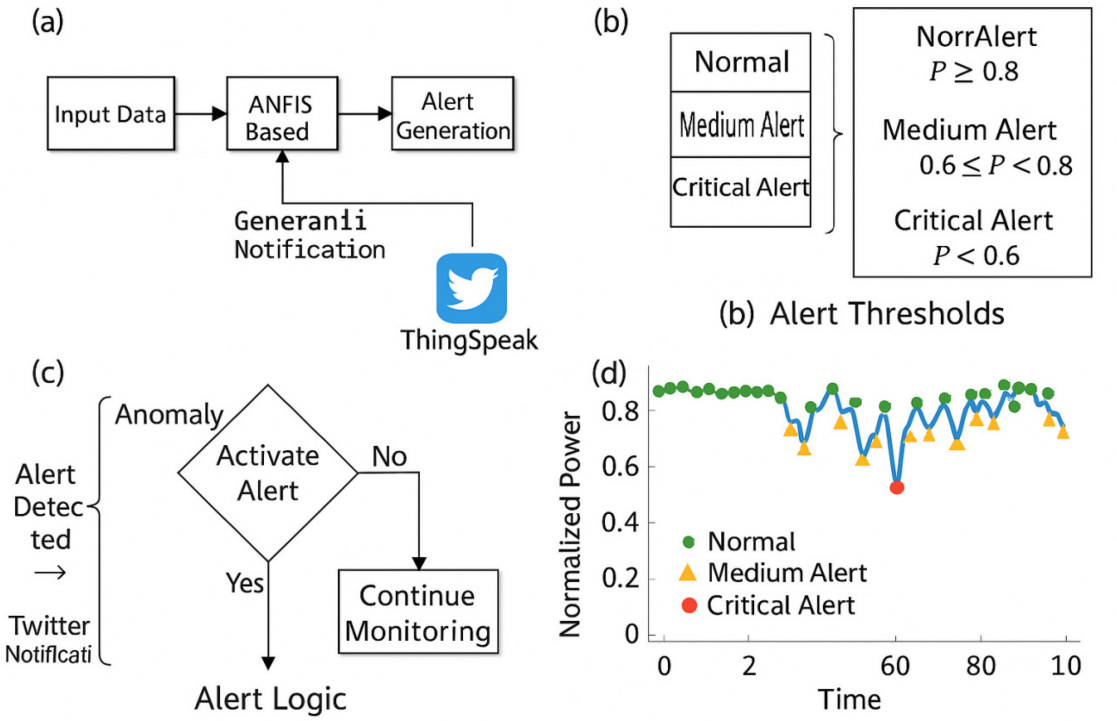

Figure 10. IoT-based real-time monitoring and anomaly detection process: (a) General architecture of the monitoring system, (b) alert generation and Twitter notification mechanism, (c) decision flow for anomaly detection, and (d) temporal evolution of normalized power output with highlights alert events

Comparative Performance Evaluation

The comparative performance evaluation, succinctly summarized in **Figure 11**, validates the efficacy of the ANFIS model against conventional machine learning approaches, including Linear Regression, Support Vector Machines (SVR), and Gradient Boosting. While all models demonstrated a commendable capacity to predict Pmax_norm, the ANFIS system consistently exhibited superior or comparable performance in terms of MAE, MSE, and RMSE, positioning itself as a robust solution for this critical task.

It is paramount to underscore that, despite models such as Gradient Boosting potentially achieving similar levels of precision, ANFIS offers a pivotal advantage within this operational context: its inherent interpretability. Unlike 'black-box' models, the neuro-fuzzy architecture of ANFIS facilitates a profound understanding of the intricate relationships between input features (EL image pixel data) and the output (*P*max_norm) through transparent fuzzy rules. This level of transparency proves invaluable for field engineers and technicians, as it significantly aids in comprehending performance diagnostics and pinpointing the root causes of faults, which is a critical aspect of informed operational decision-making **[30]**.

Furthermore, regarding computational efficiency, the ANFIS model, by leveraging computationally inexpensive histogram features and a hybrid training architecture, proves particularly well-suited for real-time monitoring environments. Its ability to operate efficiently

with comparatively smaller datasets and its reduced reliance on intensive computing infrastructure, when contrasted with certain deep neural networks or complex ensemble methods, positions it as a pragmatic and scalable solution for integration into Internet of Things (IoT) platforms and prospective edge computing deployments [31].

To contextualize the proposed ANFIS model within modern advancements, it is important to acknowledge that more recent approaches such as Random Forest Regressors, Extreme Gradient Boosting (XGBoost), LightGBM, and shallow Convolutional Neural Networks (CNNs) applied to extracted EL features have demonstrated strong predictive capabilities in related PV diagnostics research. These models are capable of capturing complex nonlinearities and have been adopted in recent literature for defect characterization and power prediction.

While the present work does not include these models in the quantitative comparison to avoid speculative results beyond the scope and constraints of the dataset, their relevance is recognized. Accordingly, Section Future Work outlines the planned integration of these modern techniques for a broader benchmarking analysis. This ensures that the comparative framework can be expanded in future studies while maintaining scientific rigor and reproducibility in the current manuscript.

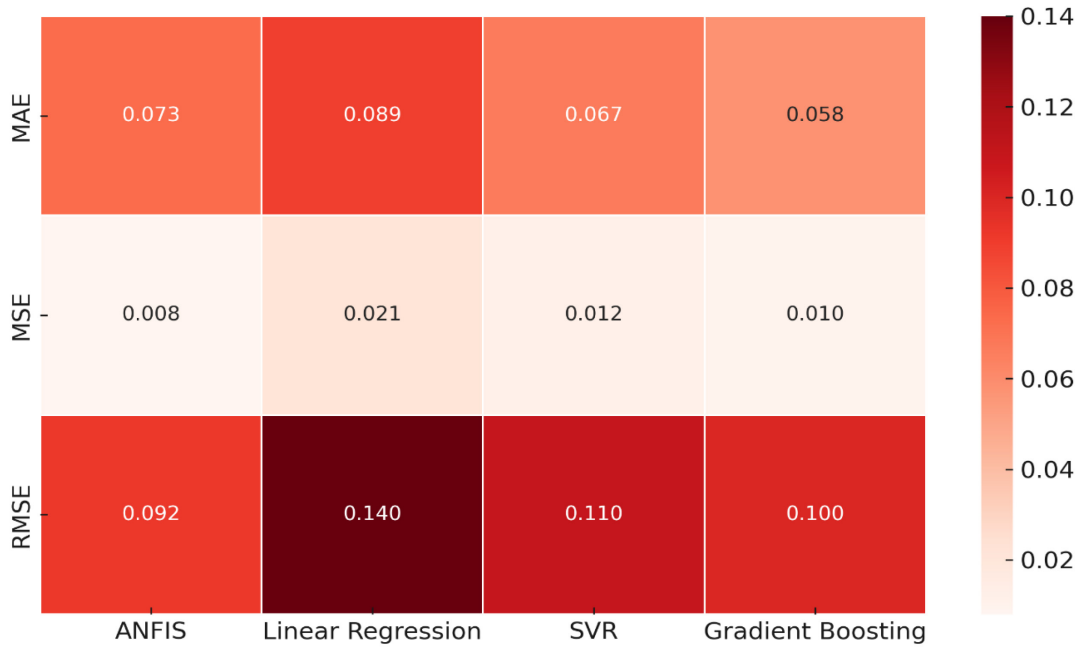

Figure 11. Heatmap visualization of predictive model error metrics. Darker red tones indicate higher error values, while lighter shades represent lower errors. The heatmap displays MAE, MSE, and RMSE for ANFIS, Linear Regression, SVR, and Gradient Boosting models, providing a comparative assessment of their predictive accuracy

The integration of electroluminescence (EL) imaging with electrical characterization data represents a synergistic approach that substantially enhances the diagnostic precision of photovoltaic (PV) systems. While EL imaging alone captures spatial degradation patterns such as cracks, shunts, or potential-induced degradation, it does not fully describe their electrical consequences. By combining EL derived pixel intensity distributions with I - V curve data, the proposed framework establishes a quantitative mapping between visual defect signatures and real performance losses. This hybridization significantly improves predictive accuracy and robustness, as it simultaneously considers morphological and electrical dimensions of PV cell behavior, reducing uncertainty compared to purely image - based or electrical only methods [32].

When contrasted with traditional machine learning models such as Linear Regression, Support Vector Regression (SVR), and Gradient Boosting, the proposed ANFIS model

achieved a superior balance between interpretability and predictive performance. While deep learning approaches such as convolutional neural networks (CNNs) can yield marginally higher accuracy in large-scale image datasets, they often lack transparency and demand greater computational resources [33]. In contrast, the neuro - fuzzy structure of ANFIS offers clear interpretability through linguistic rules, allowing engineers to trace performance degradation back to specific visual and electrical causes. This explainable framework is crucial for real world PV diagnostics, where understanding the nature of a fault is as important as detecting it [34].

LIMITATIONS

The applicability of the proposed ANFIS-based framework is constrained by several technical and experimental factors that warrant consideration. The model was trained using data obtained exclusively under controlled laboratory conditions, which minimizes noise but does not replicate the environmental variability encountered in real PV installations. Consequently, its predictive reliability under fluctuating irradiance, temperature, or aging effects remains to be verified through extended field deployment.

The study is limited to crystalline silicon technologies monocrystalline and polycrystalline cells whose electroluminescence characteristics differ from those of thin-film or perovskite materials. This restricts the model's generalizability to emerging PV architectures that exhibit distinct degradation mechanisms.

From a computational standpoint, while the ANFIS approach offers moderate complexity, scaling it for large arrays or real-time cloud integration may introduce latency and data throughput challenges. Efficient implementation on edge devices and optimization of inference routines is required to ensure low-latency monitoring in distributed PV systems. Finally, although the dataset provides robust coverage of representative defect types, its size and homogeneity may limit model adaptability to diverse field conditions. Future studies should address these aspects through larger, heterogeneous datasets incorporating real environmental variations.

Additionally, the comparative evaluation in this study focused on classical and interpretable machine learning models. Although recent approaches such as Random Forests, XGBoost, LightGBM, and lightweight CNN architectures may offer improved accuracy, they were not included in the present analysis to maintain methodological consistency and avoid generating results beyond the validated dataset. Their incorporation in future work is anticipated to strengthen the benchmarking landscape.

CONCLUSIONS AND FUTURE WORK

This study proposed an intelligent framework for estimating the maximum power point (MPP) of crystalline silicon photovoltaic (PV) cells through the integration of electroluminescence (EL) imaging and electrical characterization data. By combining spatially resolved EL features with *I–V* curve parameters, the model established a quantitative link between visual degradation patterns and actual electrical performance, substantially enhancing diagnostic precision and interpretability.

The Adaptive Neuro-Fuzzy Inference System (ANFIS) demonstrated superior predictive accuracy among the evaluated methods, achieving an RMSE of 0.092, outperforming Support Vector Regression (RMSE = 0.11), Gradient Boosting (RMSE = 0.10), and Linear Regression (RMSE = 0.14). This performance confirms the model's ability to capture nonlinear dependencies between EL-derived features and PV cell efficiency, while maintaining transparency through interpretable fuzzy inference rules. The synergy between advanced image preprocessing and hybrid neuro-fuzzy modeling provides a non-invasive, explainable, and computationally efficient diagnostic framework suitable for real-time PV monitoring applications.

Future research directions will focus on extending this framework beyond the single-cell level to include full photovoltaic panels and complete PV systems operating under real environmental conditions, with the objective of validating the scalability and generalization capacity of the ANFIS-based approach. In parallel, the benchmarking landscape will be broadened to include more advanced learning models such as Random Forests, XGBoost, LightGBM, and compact convolutional neural networks applied to EL-derived featuresto enable a deeper exploration of nonlinear behaviors and obtain complementary insights relative to the ANFIS architecture. Additionally, the integration of bio-inspired optimization algorithms, including Particle Swarm Optimization (PSO), Genetic Algorithms (GA), and Ant Colony Optimization (ACO), will be investigated to adaptively tune the ANFIS parameters and membership functions.These techniques are expected to enhance the system's adaptability, convergence speed, and robustness against non-stationary effects such as irradiance fluctuations, temperature variations, aging degradation, and partial shading.

Furthermore, future work will include a multi-objective optimization strategy aimed at improving key performance metrics, including prediction accuracy, computational efficiency, and fault detection sensitivity. The deployment of the optimized ANFIS model on edge-computing hardware platforms (e.g., Raspberry Pi, Jetson Nano, or ESP32) will also be evaluated to enable real-time, in-situ diagnostics without continuous cloud dependency. These advancements will contribute to the development of self-adaptive, scalable, and energy-efficient PV health monitoring systems, aligning with the growing demand for sustainable and intelligent renewable energy infrastructures.

ACKNOWLEDGMENTS

The authors would like to express their sincere appreciation to the Institute of Renewable Energy at the National Autonomous University of Mexico (UNAM) for its valuable support. Special acknowledgment is extended to SECIHTY and MINCIENCIAS for the doctoral scholarship provided. This research was funded by the Colombian Government through the project SGR BPIN 2024000100089. The authors also acknowledge the University of Valladolid and the research personnel who actively contributed to the acquisition and processing of the data employed in this study. MAMF was supported by the UNAM Postdoctoral Program (POSDOC).

NOMENCLATURE

I	current	[A]
P	power	[kW]
V	voltage	[V]
T	temperature	[°C]

Abbreviations

AIoT	Artificial Intelligence of Things
ANFIS	Adaptive Neuro-Fuzzy-Inference System
EL	Electroluminescence
MAE	Mean Absolute Error
MSE	Mean Squared Error
PID	Potential-Induced Degradation
PV	Photovoltaic Cell

REFERENCES

1. M. Wetzel, H. C. Gils, and V. Bertsch, "Green energy carriers and energy sovereignty in a climate neutral European energy system," *Renew Energy*, vol. 210, 2023, https://doi.org/10.1016/j.renene.2023.04.015.

2. Abdulrahman Mohammad, Mudhar Al-Obaidi, Hassan Dakkama, and Haitham Bahlol, "Modelling and optimisation of solar photovoltaic power using response surface methodology," *Journal of Sustainable Development of Energy, Water and Environment Systems*, vol. 12, no. 4, pp. 1–16, Dec. 2024, https://doi.org/10.13044/j.sdewes.d12.0519.
3. L. D. Jathar *et al.*, "Comprehensive review of environmental factors influencing the performance of photovoltaic panels: Concern over emissions at various phases throughout the lifecycle," *Environmental Pollution*, vol. 326. 2023, https://doi.org/10.1016/j.envpol.2023.121474.
4. H. Abdulla, A. Sleptchenko, and A. Nayfeh, "Photovoltaic systems operation and maintenance: A review and future directions," *Renewable and Sustainable Energy Reviews*, vol. 195. 2024, https://doi.org/10.1016/j.rser.2024.114342.
5. A. O. Ali *et al.*, "Advancements in photovoltaic technology: A comprehensive review of recent advances and future prospects," *Energy Conversion and Management: X*, vol. 26, p. 100952, Apr. 2025, https://doi.org/10.1016/J.ECMX.2025.100952.
6. "Scopus - Analyze search results n.d.," Apr. 20, 2025, https://www.scopus.com/term/analyzer.uri?sort=plf-f&src=s&sid=0cd80006d63d2734fa3ec3efe4790456&sot=a&sdt=a&sl=124&s=TITLE-ABS-KEY%28artificial+AND+intelligence+AND+photovoltaic+AND+cells+AND+power+AND+output+AND+prediction%29+AND+PUBYEAR+%3e+1999&origin=resultslist&count=10&analyzeResults=Analyze+results, [Accessed: Apr. 19, 2025].
7. Syafii Syafii, Krismadinata Krismadinata, Fahmi Fahmi, Farah Azizah, and Imra Nur Izrillah, "Enhancing Electric Vehicle Charging Stations through Internet of Things Technology for Optimizing Photovoltaic and Battery Storage Integration," *Journal of Sustainable Development of Energy, Water and Environment Systems*, vol. 13, no. 4, pp. 1–15, Dec. 2025, https://doi.org/10.13044/j.sdewes.d13.0609.
8. E. H. Sepúlveda-Oviedo, L. Travé-Massuyès, A. Subias, M. Pavlov, and C. Alonso, "Fault diagnosis of photovoltaic systems using artificial intelligence: A bibliometric approach," *Heliyon*, vol. 9, no. 11, p. e21491, Nov. 2023, https://doi.org/10.1016/J.HELIYON.2023.E21491.
9. A. Thakfan and Y. Bin Salamah, "Artificial-Intelligence-Based Detection of Defects and Faults in Photovoltaic Systems: A Survey," *Energies (Basel)*, vol. 17, no. 19, 2024, https://doi.org/10.3390/en17194807.
10. Q. Wei, H. Sun, J. Fan, G. Li, and Z. Zhou, "AIoT-Based Visual Anomaly Detection in Photovoltaic Sequence Data via Sequence Learning," *Energies (Basel)*, vol. 17, no. 21, 2024, https://doi.org/10.3390/en17215369.
11. R. Bin Mofidul, S. S. Alam, A. Chakma, B. D. Chung, and Y. M. Jang, "Predictive Maintenance in Photovoltaic Systems Using Ensemble ML Empirical Analysis," in *International Conference on Ubiquitous and Future Networks, ICUFN*, 2023, vol. 2023-July, https://doi.org/10.1109/ICUFN57995.2023.10199326.
12. S. L. P, S. S, and M. S. Rayudu, "IoT based solar panel fault and maintenance detection using decision tree with light gradient boosting," *Measurement: Sensors*, vol. 27, p. 100726, Jun. 2023, https://doi.org/10.1016/J.MEASEN.2023.100726.
13. H. F. Mateo-Romero *et al.*, "Enhancing photovoltaic cell classification through mamdani fuzzy logic: a comparative study with machine learning approaches employing electroluminescence images," *Progress in Artificial Intelligence*, vol. 14, no. 1, pp. 49–59, 2025, https://doi.org/10.1007/s13748-024-00353-w.
14. U. Hijjawi, S. Lakshminarayana, T. Xu, G. Piero Malfense Fierro, and M. Rahman, "A review of automated solar photovoltaic defect detection systems: Approaches, challenges, and future orientations," *Solar Energy*, vol. 266, p. 112186, Dec. 2023, https://doi.org/10.1016/J.SOLENER.2023.112186.

15. A. A. Al-Katheri, E. A. Al-Ammar, M. A. Alotaibi, W. Ko, S. Park, and H. J. Choi, "Application of Artificial Intelligence in PV Fault Detection," *Sustainability (Switzerland)*, vol. 14, no. 21, 2022, https://doi.org/10.3390/su142113815.
16. F. Conte, F. D'Antoni, G. Natrella, and M. Merone, "A new hybrid AI optimal management method for renewable energy communities," *Energy and AI*, vol. 10, p. 100197, Nov. 2022, https://doi.org/10.1016/J.EGYAI.2022.100197.
17. M. E. C. dela and H.-C. L. and G.-R. M. Á. and C.-P. V. and A.-G. V. and M.-S. Ó. and G.-S. S. Mateo-Romero Hector Felipe and Rosa, "Estimation of the Performance of Photovoltaic Cells by Means of an Adaptative Neural Fuzzy Inference Model," in *Smart Cities*, 2024, pp. 174–188, https://doi.org/10.1007/978-3-031-52517-9_12.
18. M. E. Carbono dela Rosa, J. Gómez, A. Ospino, J. M. Sánchez-De-La-Hoz, and C. Robles, "Enhanced Spectral Analysis Approaches for Predicting Critical Failures in Lithium-Ion Batteries: A Wavelet-Based Framework," *Journal of Sustainable Development of Energy, Water and Environment Systems*, vol. 13, no. 4, pp. 1–16, Dec. 2025, https://doi.org/10.13044/j.sdewes.d13.0613.
19. M. Bildirici, F. Kayıkçı, and Ö. Ö. Ersin, "Industry 4.0 and Renewable Energy Production Nexus: An Empirical Investigation of G20 Countries with Panel Quantile Method," *Sustainability (Switzerland)*, vol. 15, no. 18, 2023, https://doi.org/10.3390/su151814020.
20. K. Ukoba, K. O. Olatunji, E. Adeoye, T.-C. Jen, and D. M. Madyira, "Optimizing renewable energy systems through artificial intelligence: Review and future prospects," *Energy & Environment*, vol. 35, no. 7, pp. 3833–3879, 2024, https://doi.org/10.1177/0958305X241256293.
21. R. Selvaraj, V. M. Kuthadi, and S. Baskar, "Smart building energy management and monitoring system based on artificial intelligence in smart city," *Sustainable Energy Technologies and Assessments*, vol. 56, 2023, https://doi.org/10.1016/j.seta.2023.103090.
22. H. F. Mateo Romero, "Employing artificial intelligence techniques for the estimation of energy production in photovoltaic solar cells based on electroluminescence images," Universidad de Valladolid, Valladolid, Spain, 2024.
23. M. E. C. dela Rosa *et al.*, "Detection of failures in electrode-photovoltaic cell junctions through two-dimensional wavelet analysis of electroluminescence images," *Renewable Energies*, vol. 2, no. 2, p. 27533735241304090, 2024, https://doi.org/10.1177/27533735241304090.
24. A. V. Patel, L. McLauchlan, and M. Mehrubeoglu, "Defect Detection in PV Arrays Using Image Processing," 2020, https://doi.org/10.1109/CSCI51800.2020.00304.
25. T. M. S. Kumar, S. Sharma, C. P. Kurian, S. M. Varghese, and A. M. George, "Adaptive Neuro-fuzzy Control of Solar-Powered Building Integrated with Daylight-Artificial Light System," 2020, https://doi.org/10.1109/PESGRE45664.2020.9070406.
26. M. Vakili, M. Yahyaei, J. Ramsay, P. Aghajannezhad, and B. Paknezhad, "Adaptive neuro-fuzzy inference system modeling to predict the performance of graphene nanoplatelets nanofluid-based direct absorption solar collector based on experimental study," *Renew Energy*, vol. 163, pp. 807–824, Jan. 2021, https://doi.org/10.1016/J.RENENE.2020.08.134.
27. A. Abubakar, M. M. Jibril, C. F. M. Almeida, M. Gemignani, M. N. Yahya, and S. I. Abba, "A Novel Hybrid Optimization Approach for Fault Detection in Photovoltaic Arrays and Inverters Using AI and Statistical Learning Techniques: A Focus on Sustainable Environment," *Processes*, vol. 11, no. 9, 2023, https://doi.org/10.3390/pr11092549.
28. D. Balakrishnan, J. Raja, M. Rajagopal, K. Sudhakar, and K. Janani, "An IoT-Based System for Fault Detection and Diagnosis in Solar PV Panels," in *E3S Web of Conferences*, 2023, vol. 387, https://doi.org/10.1051/e3sconf/202338705009.
29. B. Li, S. B. Fesseha, S. Chen, and Y. Zhou, "Real-Time Solar Power Generation Scheduling for Maintenance and Suboptimally Performing Equipment Using Demand

Response Unified with Model Predictive Control," *Energies (Basel)*, vol. 17, no. 13, 2024, https://doi.org/10.3390/en17133212.

30. R. A. Eltuhamy, M. Rady, E. Almatrafi, H. A. Mahmoud, and K. H. Ibrahim, "Fault Detection and Classification of CIGS Thin-Film PV Modules Using an Adaptive Neuro-Fuzzy Inference Scheme," *Sensors*, vol. 23, no. 3, 2023, https://doi.org/10.3390/s23031280.
31. A. Gopi, P. Sharma, K. Sudhakar, W. K. Ngui, I. Kirpichnikova, and E. Cuce, "Weather Impact on Solar Farm Performance: A Comparative Analysis of Machine Learning Techniques," *Sustainability (Switzerland)*, vol. 15, no. 1, 2023, https://doi.org/10.3390/su15010439.
32. T. Fuyuki, H. Kondo, Y. Kaji, A. Ogane, and Y. Takahashi, "Analytic findings in the electroluminescence characterization of crystalline silicon solar cells," *J Appl Phys*, vol. 101, no. 2, 2007, https://doi.org/10.1063/1.2431075.
33. M. A. Ebied, A. Munshi, S. A. Alhuzali, M. M. El-sotouhy, A. I. Shehta, and M. S. Elborlsy, "Advanced deep learning modeling to enhance detection of defective photovoltaic cells in electroluminescence images," *Sci Rep*, vol. 15, no. 1, p. 31640, 2025, https://doi.org/10.1038/s41598-025-14478-y.
34. U. Kumar, S. Mishra, and K. Dash, "An IoT and Semi-Supervised Learning-Based Sensorless Technique for Panel Level Solar Photovoltaic Array Fault Diagnosis," *IEEE Trans Instrum Meas*, vol. 72, 2023, https://doi.org/10.1109/TIM.2023.3287247.

Paper submitted: 23.07.2025
Paper revised: 30.11.2025
Paper accepted: 10.12.2025